

Nanophase Structure and Diffusion in Swollen Perfluorosulfonate Ionomer: An NMR Approach

Marcus V. Giotto, Jinghui Zhang, Paul T. Inglefield, Wen-Yang Wen, and Alan A. Jones*

Carlson School of Chemistry and Biochemistry, Clark University, Worcester, Massachusetts 01610

Received December 20, 2002; Revised Manuscript Received April 4, 2003

ABSTRACT: Fluorine-19 NMR was used to study the structure and mobility of the perfluorosulfonate ionomer Nafion (Dupont trademark) in the presence of dimethyl methylphosphonate (DMMP). Fluorine-19 resonances arising from the ionomeric side chain narrowed rapidly with increasing DMMP content while the resonances arising from the perfluoroethylene backbone units remained broad. The plasticization of the side chains indicates that the DMMP is primarily associated with this structural unit which forms its own nanophase in Nafion. To further characterize the morphological structure, fluorine-19 spin diffusion experiments between the side chain and backbone resonances were performed. At low DMMP content, swelling of the pendant group domain is observed while at higher concentrations an unusual change in the spin diffusion indicates the development of a new morphology consisting of larger domains associated with the pendant group plus DMMP. To augment information on this system, proton pulse field gradient experiments were performed as a function of concentration and temperature to obtain DMMP self-diffusion constants. In the same concentration range where morphological change occurred, there was a rapid rise in translational mobility of the DMMP. This reflects the influence of the new larger domains which allow longer range motion of DMMP with fewer obstructions from the backbone domains which are relatively impermeable to DMMP. A fraction of the smaller domains originally present in dry Nafion remain even at high levels of DMMP, indicating an inability of all of the Nafion to undergo the morphological transition to the larger domains.

Introduction

The morphological structure of the perfluorosulfonate ionomer Nafion (Dupont trademark) and the transport of ions and low molecular weight compounds through this polymer have been the subject of many investigations.^{1,2} Interest arises from the many potential and existing applications of this polymer as a membrane material in electrochemistry, sensors, fuel cells, and chemical protection. Transport of water and alcohols thorough Nafion is very rapid despite the general hydrophobicity of fluoropolymers. The ionic groups on the side chains are considered to provide a continuous pathway for permeation of molecules containing ionizable protons. Sometimes this pathway is described in terms of clusters and channels though this is more of a model than an established structure.³

The most common techniques used in the study of the morphology of Nafion are X-ray and neutron scattering.^{1,2} These experiments show the existence of nanometer sized clusters of the ionic groups which are particularly easily detected in metal ion neutralized forms of Nafion. Recently, fluorine-19 NMR has shown that the ionomeric side chains constitute a separate nanometer sized phase from the fluorocarbon backbone.⁴ The side chains might be considered to form an interface between the fluorocarbon backbone and the ionic or ionizable group at the end of the side chain. The poly-(fluoroethylene) backbone domains are also divided between crystalline and amorphous components.¹ This overall complex morphology is sometimes assumed to have structural or geometrical regularity: spherical clusters, lamellar domains, etc. Often these assumptions of regularity seem to be more for the purposes of data analysis than realistic aspects of the complex morphology.⁵

Scattering experiments indicate water plasticizes and swells the ionic domains^{1,2} while NMR experiments

indicate alcohols swell and plasticize the ionomeric side chain domains.⁴ In addition, ethanol plasticizes part of the backbone domain and induces a more significant morphological change than just swelling.⁴ At low water content, less than 20 wt %, the morphology of dry Nafion is retained with swelling of the ionomeric side chain domains.^{4,6} Ethanol induces a change from the dry Nafion structural repeat length even at these low concentrations.⁴ In the presence of water/ethanol mixtures or water at high temperatures,^{6–8} a significant change in the morphological structure of Nafion is also observed. At low concentrations the ionic clusters can be considered as reverse micelles surrounded by fluoropolymer.⁶ At high concentrations of water produced by using high temperatures, there is a reversal of the morphology where the predominant phase is the swollen ionic component, and the fluoropolymer is considered to be cylinders or ribbons coated with the ionic groups in a normal micelle structure.^{6,7} Of course, these structural changes would affect the nature of the translational motion of the low molecular weight compound through the complex morphology.

Hydrocarbons are rather insoluble in Nafion and consequently do not readily swell or permeate Nafion films. On the other hand, polar organics not containing hydroxyl groups or other ionizable protons can be highly soluble in Nafion. It is the goal of this report to characterize diffusion and the morphological structure of Nafion swollen with such penetrants using NMR. In addition, the changes in the nature of the translational motion of the polar organic molecules will be correlated with the morphological changes.

The penetrant chosen for this study is dimethyl methylphosphonate (DMMP), which swells Nafion to a level of more than 60 wt % (defined as 100 times weight DMMP divided by weight polymer plus weight DMMP). Such a high level of DMMP uptake seems likely to cause

morphological changes since at this level it constitutes a majority of the system. DMMP is structurally similar to nerve agents and pesticides although is itself not toxic. Nafion is a possible material for applications in chemical protection since it readily transports water while acting as a barrier for many organics. In this regard, information on the diffusion of DMMP in Nafion and the effect of DMMP on Nafion morphology could be helpful in evaluating Nafion for chemical protection applications.

Pulse field gradient (PFG) NMR is used to measure the self-diffusion constants of DMMP in Nafion.⁹ This technique can also detect characteristics of translational motion such as restricted or tortuous diffusion^{10,11} which might be encountered in a multiphase medium where only one of the phases is accessible to the penetrant. The PFG measurements are made as a function of concentration and temperature.

A key question is the location of the DMMP in the various morphological environments of the phase-segregated Nafion structure. Does DMMP dissolve only in the perfluoroether side chain domains or only in the fluorocarbon domains? Perhaps it is uniformly distributed in all phases. When it becomes the majority of the system, what is the relationship to the Nafion morphology? To determine this, the static fluorine-19 line shape⁴ will be observed as a function of DMMP concentration. The presence of low molecular weight penetrant in a morphological domain is expected to plasticize the polymer in that domain. The static spectrum consists principally of two lines: one for the side chain and one for the backbone.⁴ In previous studies it was shown that water slightly plasticizes the side-chain domain while ethanol significantly plasticizes the side-chain domain and begins to plasticize the backbone domain at higher ethanol concentrations.⁴ In a similar fashion, the presence or absence of DMMP in these two domains should be indicated by changes in the static line width.

Fluorine-19 spin diffusion under conditions of magic angle spinning will then be used to monitor changes in morphology⁴ as a function of sorbed DMMP. At spinning speeds of 10 kHz and higher, the side chain and backbone resonances are well resolved.⁴ The resonance associated with fluorines on the side chain will be selectively inverted, and the return of the magnetization to spin-spin equilibrium will be monitored. Assuming a value for the spin diffusion constant allows for a determination of the repeat length of the morphological structure associated with the backbone and side chain.¹² On the basis of the relative amount of the two morphological components, the overall repeat length can be broken down into a size for each domain.

Thus, three experiments will be performed to ascertain diffusion constants, location of the penetrant within the morphological domains, and size of the two major domains. An interpretation will be sought which leads to a consistent description of the three measurements as a function of the concentration of DMMP. In total, the interplay between diffusion and structural results should lead to an overall understanding of the interaction of this penetrant in Nafion and contribute to a further understanding of transport behavior and structure in Nafion.

Experimental Section

Nafion-115 in the hydrogen (acid) form was purchased from Aldrich. The equivalent weight per ionic group was 1100 g. Samples were also prepared with Nafion 117, which also has

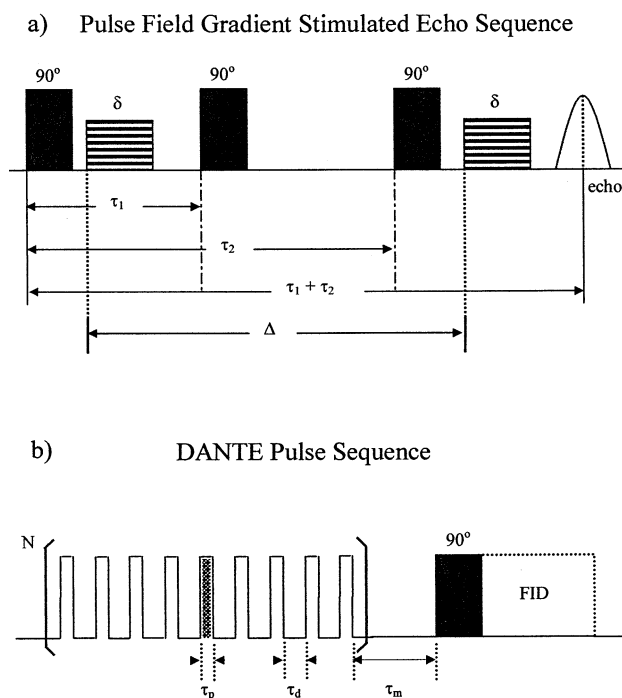


Figure 1. (a) Pulse sequence used for the measurement of proton translational diffusion. The gradient pulse width, δ , is typically 1 ms, and the time over which diffusion occurs, Δ , can be varied from 1 to 1000 ms but typically it was set at 50 ms. (b) Pulse sequence used for performing fluorine-19 spin-diffusion experiments. The number of small angle pulses, N , was in the range from 8 to 12. The small angle pulse width, τ_p , and the pulse interval, τ_d , ranged from 0.6 to 0.9 μ s and 18 to 33 μ s, respectively. The mixing time, τ_m , was varied from 100 μ s to 100 ms. The 90° pulse was 2 μ s, the delay time 5 s, and the acquisition time 20 ms.

an equivalent weight of 1100 g. The Nafion was cut to produce pieces suitable for magic angle spinning experiments and vacuum-dried for several days at a temperature of 60 °C. The Nafion was then swollen to different levels with DMMP. Samples were prepared by adding a specific amount of DMMP to Nafion in a 5 mm NMR tube, by immersion, or by swelling Nafion with DMMP vapor. They were chilled with liquid nitrogen and then degassed and flame-sealed in NMR tubes. No difference was noted between the results of the NMR experiments among these different preparations. Samples equilibrated for a period of days to weeks before measurement and no changes with time were observed after this length of equilibration.

PFG measurements were made on a Varian Inova 400 MHz wide bore NMR spectrometer in an 8 mm direct detection probe with high gradient capability (1000 G/cm) from Doty Scientific. Glass spacers were used in the NMR tube to center the sample of the correct size in the region of the radio frequency and gradient coils. Using proton NMR, the apparent diffusion constant of the penetrant, D , was measured as a function of the time, Δ , over which self-diffusion occurs in the stimulated echo pulse sequence shown in Figure 1a. Only the initial decay of echo amplitude was monitored, typically to a level of about 50% of the original amplitude. At a given time, Δ , the quantity $q = \gamma \delta g / 2\pi$ was varied by changing the gradient amplitude, g , from 0 to 800 G/cm for the Doty probe. The time, Δ , ranged from 2 ms to 1 s. A fixed value of δ , the length of the gradient pulses, of 1 ms was used for a given determination of the apparent diffusion constant. The apparent diffusion constant at a given value of Δ is calculated from the slope of a plot of the logarithm of the echo amplitude vs q^2 . In this system, D was not found to depend strongly on Δ so only a single value of D is reported for a particular concentration and temperature. The uncertainty in a given value of the apparent diffusion constant is about $\pm 5\%$.

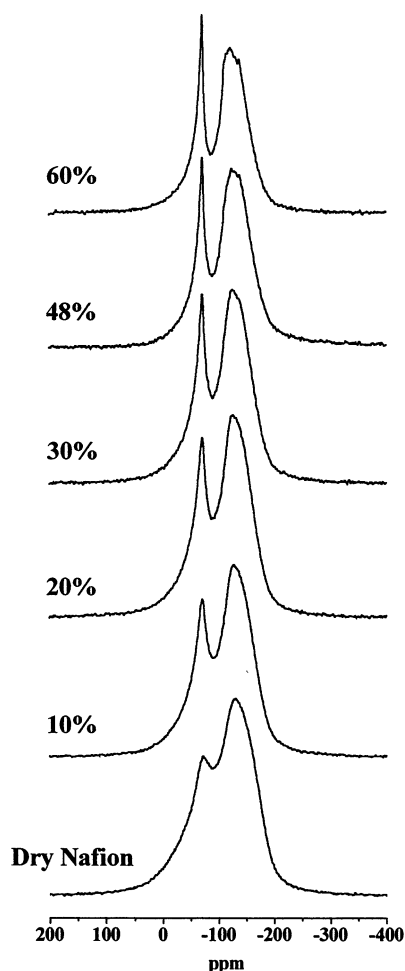


Figure 2. Static fluorine-19 wide-line spectra of Nafion with various amounts of DMMP.

All fluorine-19 NMR experiments were performed on the Varian Inova 400 MHz wide bore NMR spectrometer in a 2.5 mm MAS probe. The fluorine-19 spin diffusion measurements were made at a spinning speed of 10 kHz with care taken so that spinning sidebands did not overlap the center band resonances involved in the magnetization exchange. One set of spin diffusion measurements was made as a function of spinning speed between 5 and 20 kHz to check the effects of spinning on spin diffusion. The fluorine-19 $\pi/2$ pulse width was typically 2 μ s, and a DANTE sequence was used to selectively invert one of the resonances in order to create a magnetization gradient.

The pulse sequence used to observe spin diffusion is shown in Figure 1b. In the experiments reported here the OCF_2 and CF_3 resonances of the pendant group at about -80 ppm relative to CFCl_3 were inverted, and spin exchange to the CF_2 of the backbone at about -120 ppm then occurred. A series of spectra were acquired as a function of time after the inversion to monitor the return to spin-spin equilibrium. Typically, spin-spin equilibrium was reached in 50 ms, which was considerably shorter than the spin-lattice relaxation times which are on the order of a second or longer. Static fluorine-19 spectra were taken in the MAS probe with the bearing pressure turned off to prevent spinning.

Results and Interpretation

Fluorine-19 Spectra. The static or nonspinning fluorine-19 spectra in Figure 2 indicate dramatic narrowing of the resonance near -80 ppm and little change of the resonance near -120 ppm. This is clear evidence for plasticization of the pendant group domain while the poly(fluoroethylene) or backbone domain remains un-

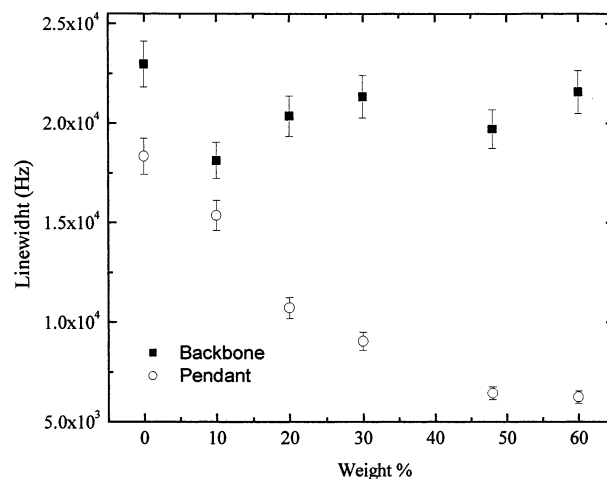


Figure 3. Line width of the fluorine-19 resonances. The circles are for the pendant group, and the squares are for the perfluoroethylene backbone resonances. The line widths were determined by simulating the line shapes shown in Figure 2.

changed. Figure 3 is a plot of the line width of the -80 ppm resonance determined from line shape simulation as a function of DMMP concentration. Over the concentration range covered, the line narrows by about a factor of 4. The resonance at -120 ppm remains essentially unchanged in the line shape simulation as the concentration of DMMP increases. The conclusion drawn from these line shapes is that the DMMP is primarily dissolved in the pendant group domain. At low concentrations of water (<20 wt %), only the resonance associated with the pendant group narrowed but to a much smaller extent than that produced by DMMP.⁴ In the case of ethanol,⁴ the pendant group resonance narrowed significantly, but the backbone resonance also narrowed at high ethanol concentrations. The behavior of DMMP differs from either of the two other penetrants studied.

Fluorine-19 Spin Diffusion. Normalized representative spin diffusion plots following the format used by VanderHart¹² are shown in Figure 4 for dry Nafion as well as 10, 48 and 60 wt % DMMP (wt % DMMP = {wt DMMP/[wt Nafion + wt DMMP]} \times 100). The interpretation of these spin diffusion plots can now be considered using the information gained from the static line shapes. Typical recovery curves are shown in Figure 4, and the usual analysis^{4,12} involves extrapolating the initial decay to the time axis to obtain a value of $t_{sd}^{1/2}$. For low concentrations of DMMP less than 20 wt % this approach works reasonably well and parallels the results obtained earlier for water in Nafion: that is, the value of $t_{sd}^{1/2}$ increases as the concentration of DMMP increases. The repeat length, L , of the morphological structure assumed to consist of two domains can be calculated from $t_{sd}^{1/2}$ according to the equation

$$L = [4(t_{sd}^{1/2})(D_A D_B)^{1/2}(\rho^{F_A} f_A + \rho^{F_B} f_B) / [f_A f_B \pi^{1/2}(\rho^{F_A} D_A^{1/2} + \rho^{F_B} D_B^{1/2})]] \quad (1)$$

where ρ^{F_A} is the fluorine-19 spin density in domain A, ρ^{F_B} is the fluorine-19 spin density in domain B, D_A is the spin diffusion constant in domain A, D_B is the spin diffusion constant in domain B, f_A is the volume fraction of domain A, and f_B is the volume fraction of domain B. Note that the symbol F refers to fluorine in this equation.

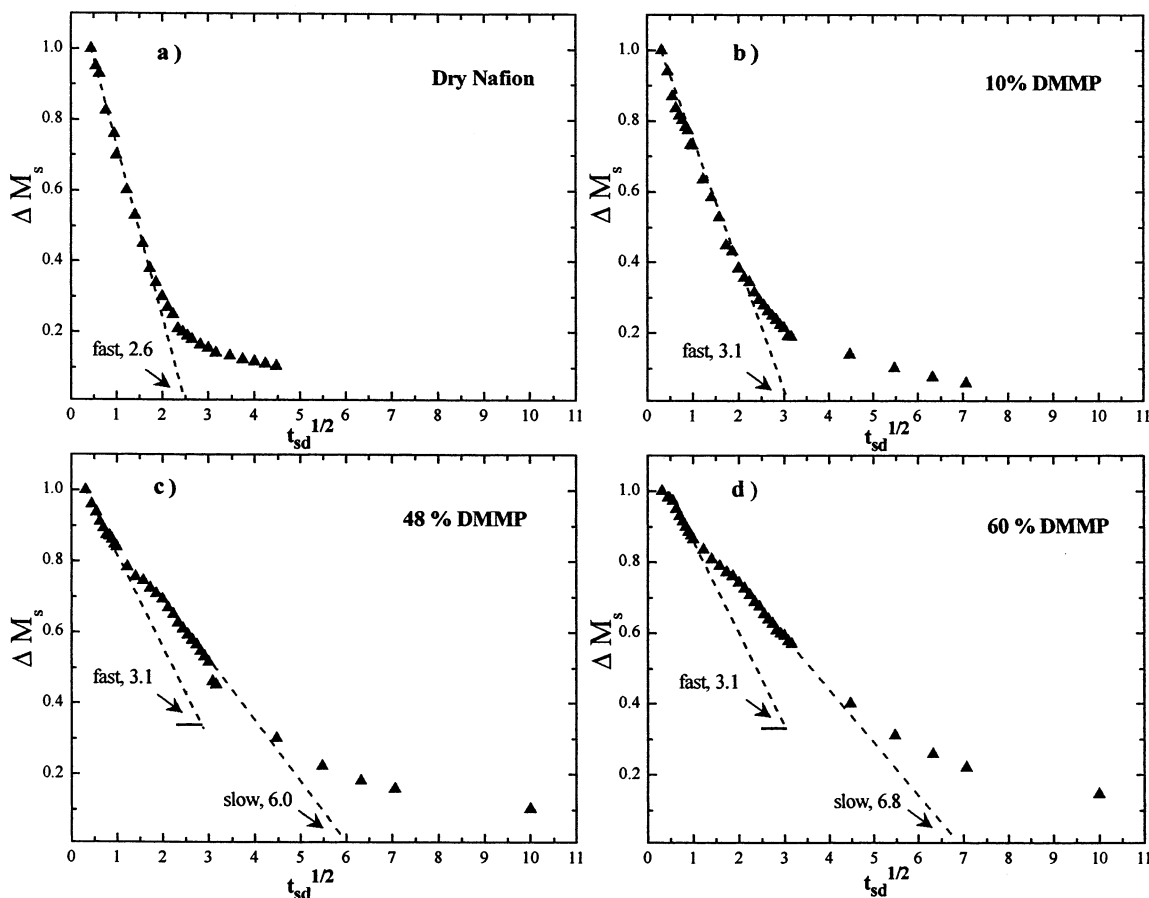


Figure 4. Representative standard spin diffusion plots¹² at concentrations of 0, 10, 48, and 60 wt % DMMP in Nafion. The return of the normalized pendant group magnetization is plotted against the square root of time following the creation of the magnetization gradient. Note the two-component nature of the return to spin–spin equilibrium at high concentrations of DMMP.

The pendant group domain will be considered as the A domain, and the backbone group domain will be considered as the B domain. The domain size is given by the product of f and L . For dry Nafion 117, the volume fraction corresponds to the weight of the pendant group, 363, divided by the equivalent weight of 1100. For the swollen Nafion, the volume associated with a weight of pendant chain is calculated assuming a density of 2.0 g/cm³. The same density is used for the backbone domains. Simple additivity of volumes is assumed so that

$$f_A = (V_{\text{solvent}} + V_{\text{pendant}}) / (V_{\text{solvent}} + V_{\text{pendant}} + V_{\text{backbone}}) \quad (2)$$

This equation also assumes that all of the DMMP is in the pendant group domain. The spin diffusion constant will be assumed as 0.62 nm²/s, which is the value for a rigid organic hydrocarbon^{4,12} given that fluorine interatomic distances are similar in fluorocarbons and hydrocarbons as are the gyromagnetic ratios. In an earlier report on Nafion, potential complications arising from narrowing of the resonances and possible changes in the spin diffusion constant were discussed.⁴ These same issues are in play with DMMP in Nafion, but the approach remains as outlined here.

This approach could be continued for concentrations of DMMP greater than 20 wt % by always using the initial part of the curve in the standardized spin diffusion plot. However, there is an unusual qualitative feature in the plots for higher concentrations which is

readily apparent in Figure 4 for a concentration of 48 and 60 wt % DMMP. There is a distinct break in the curve after the initial decay, and a second slower decay is noted after that break.

The proposed interpretation of this unusual return to spin–spin equilibrium is that there are two different domains associated with the pendant group present at high concentrations like 60 wt %, and they are of different sizes. The two domains coexist at high concentrations but are in different spatial locations in the sample. The rapid decay is associated with a morphology that is similar to the morphology originally present in dry Nafion. This morphology has a value of L equal to 11.4 nm and a pendant domain size of 3.8 nm in the dry state. In the earlier interpretation associated with water L changed little, and the pendant domain underwent swelling. This same picture largely applies to DMMP below 20 wt %. Near room temperature water uptake is limited to about 20 wt %, but if high temperatures are employed,^{6,7} Nafion solutions can be produced; these involve a new morphology when water plus ionic pendant groups becomes the major phase. The crossover point in the case of water is about 20 wt %, and we believe a similar phenomenon is occurring with DMMP except high temperatures are not required to achieve high uptakes of DMMP. The static line shape data indicates the DMMP is primarily located in the pendant group phase. On the basis of the repeat unit structure, the pendant group is about 33% of dry Nafion. If one calculates volume fraction of solvent assuming all solvent is in the pendant group phase, then at about

Table 1. ^{19}F Spin Diffusion Results^a

wt % DMMP	% fast	$t_{\text{sd}}^{1/2}$ fast	$t_{\text{sd}}^{1/2}$ slow	L (nm) fast	L (nm) slow
0	100	2.6		11	
10	100	3.1		12	
20	80	3.1	4.6	12	13
30	75	3.2	5.6	12	16
48	50	3.2	6.0	12	15
60	55	3.1	6.8	12	18

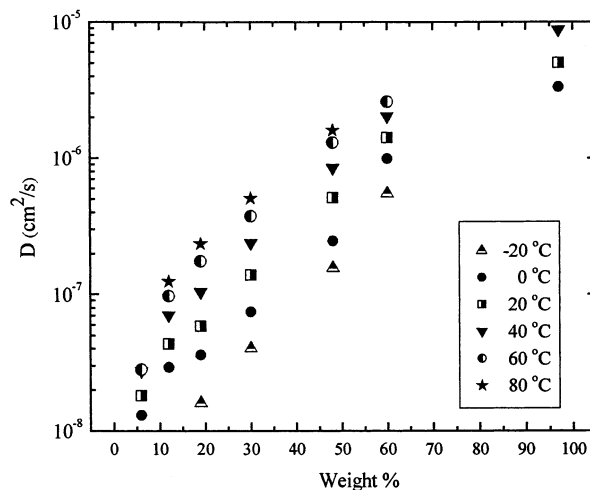
^a $t_{\text{sd}}^{1/2}$ = square root of spin-diffusion time intercept. L = overall structure repeat length.

20 wt % DMMP the volume fraction DMMP plus pendant group is about 50%, so it is becoming the major component.

To obtain a measure of the size of the new phase structure that is appearing, a more complex analysis of the spin diffusion curve is required. Essentially we want to separate the observed curve into the two components: a fast decay corresponding to a smaller pendant group phase and a slow component corresponding to a larger pendant group phase. To do this, the initial rapid decay is fit to the equation for a straight line. This component described by a straight line is then scaled and subtracted to leave only the slow component. The slow component essentially starts at a value of 2 on the square root of time axis. Table 1 lists the fraction of fast component in this analysis. The remaining slow component initial decay is then linearly extrapolated to obtain an intercept on the square root of time axis. After this intercept is determined, the slow decay curve is subtracted from the complete curve to leave an initial fast decay which can be extrapolated to obtain an intercept for the fast component. Table 1 lists the intercepts for the slow and fast components. To obtain a domain size corresponding to the fast and slow decays, assumptions must be made about the concentration of DMMP in the domain structure associated with the two components.

Since $t_{\text{sd}}^{1/2}$ for the fast component is essentially constant at all concentrations beginning with 10 wt %, the concentration in the domain associated with the fast component will be assumed to be fixed at 10 wt %. This is consistent with no further swelling of the domain associated with the fast component after a level of 10 wt % DMMP is reached. The $t_{\text{sd}}^{1/2}$ associated with the slow decay continues to increase as concentration rises, indicating that this domain continues to swell. The concentration of DMMP in this domain is larger than the overall, average concentration above 10 wt % since the concentration in the domain associated with the fast decay is fixed at 10 wt %. The concentration in the domain associated with slow decay in the spin diffusion experiment can be readily calculated since the fraction of the system that is fast and slow is determined by the spin diffusion data. The density of fluorine spins, ρ in eq 1, will be different in the two domains since the concentration of DMMP is different. The concentrations, square root of time intercepts, and the domain size, L , corresponding to the slow and fast components calculated from eq 1 are given in Table 1. Table 2 contains the size of the pendant group domain corresponding to the slow and fast decays in the spin diffusion plot as well as the values of the concentrations of DMMP and spin densities in the two domains.

In order for there to be as clear a break between the two components of the spin diffusion curve as is visible in Figure 4 for the case of 60 wt % DMMP, there must

**Figure 5.** Self-diffusion constants for DMMP in Nafion at various temperatures as a function of wt % DMMP.**Table 2.** Domain Size^a

wt % DMMP	f_A fast	$\rho^{F_A} \times 10^{22}$ ($^{19}\text{F}/\text{cm}^3$) fast	f_A slow	$\rho^{F_A} \times 10^{21}$ ($^{19}\text{F}/\text{cm}^3$) slow	P (nm) fast	P (nm) slow
0	0.33	3.3			3.8	
10	0.44	2.1			5.1	
20	0.44	2.1	0.72	6.2	5.1	9.7
30	0.44	2.1	0.80	5.0	5.3	13
48	0.44	2.1	0.81	3.0	5.3	12
60	0.44	2.1	0.80	3.2	5.1	14

^a P = pendant domain size.

be an initial flat part of the slow decay which persists to a value of about 2 on the $t^{1/2}$ scale. This corresponds to a large interface region for the slow component.^{12–14} Note that the fast component, which is the only component in dry Nafion, has a smaller initial flat part of the decay curve which corresponds to a smaller interface. The interface thickness, d_{int} , can be estimated by considering the decay curve to offset on the square root of time axis.

In relation to the overall structural repeat length L where

$$L = l_{\text{pendant}} + l_{\text{backbone}} + 2d_{\text{int}} \quad (3)$$

the interface thickness is given by

$$2d_{\text{int}} \approx \sqrt{6Dt_{\text{sd}}} \quad (4)$$

Applying this equation leads to an estimate of an interface thickness of 2 nm for the larger domain which ranges from 10 to 14 nm as concentration increases from 20 to 60 wt %. While this is only an estimate, the data indicate that the larger domain which grows in at higher concentrations involves a thicker interface.

Proton Measurements of Self-Diffusion on DMMP. As would be expected, Figure 5 indicates that diffusion becomes faster as the concentration of DMMP increases at a given temperature. In the case of water and ethanol, Fujita free volume theory could be applied to summarize the concentration dependence.⁹ For water, only the pendant group domain was plasticized so all water was considered to be located in this domain. For Nafion 117, this domain is about one-third of all of the polymer so the relevant concentration was the volume fraction of water in the pendant group domain. This led

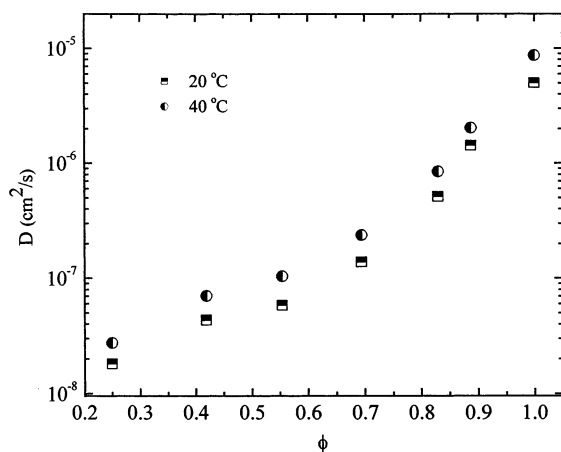


Figure 6. Self-diffusion constants plotted as a function of volume fraction for $T = 20$ and 40 °C assuming all DMMP is sorbed into the pendant group phase. Note the sharp rise in the values of D at higher concentrations.

to reasonable free volume parameters for the polymer and the solvent, so a similar strategy was attempted for DMMP since it too also only plasticizes the pendant group domain. Figure 6 shows data for the concentration dependence of diffusion constants at two representative temperatures ($T = 20$ and 40 °C) assuming all the DMMP is in the pendant group domain. The concentration dependence is distinctly non-Fujita in form and cannot be reasonably fit with a Fujita type equation. The rescaling of the concentration between weight percent in Figure 5 and volume fraction in the pendant group phase emphasizes the non-Fujita concentration dependence. The lowest three concentration points plotted in Figure 6 could be fitted to a Fujita dependence, but after a volume fraction of 0.5 the diffusion constants increase much more rapidly. A curve drawn through the first three points is concave downward which is typical of the Fujita shape, but the last three points change to a concave upward form which cannot be matched a Fujita equation. The switch from concave downward to concave upward coincides in concentration with the appearance of the larger domains in the spin diffusion plots. Considering the structural transition taking place, the rapid increase in translational diffusion above a volume fraction of about 0.5 in the pendant group domain is associated with the development of the larger pendant group domain structure. As the solvent plus pendant group phase becomes the majority of the system, a micellar rodlike or ribbonlike structure is proposed by Gebel^{6,7} where the poly(perfluoroethylene) units are surrounded by the pendant groups and solvent. In this situation where the pendant groups and solvent are the majority phase, there should be better connectivity for solvent diffusion than in the case where there is less solvent and the pendant group plus solvent is the minority domain.

If the temperature dependence of the diffusion data is considered, free volume theory could again be the starting point using the well-known WLF equation.

$$\ln\left(\frac{DT_0}{D_0T}\right) = \frac{\frac{\alpha(\phi_s)}{B_d}(T - T_0)}{\frac{f(\phi_s)}{B_d}\left(\frac{f(\phi_s)}{B_d} + \frac{\alpha(\phi_s)}{B_d}(T - T_0)\right)} \quad (5)$$

where $f(\phi_s)$ is the fractional free volume of the solution,

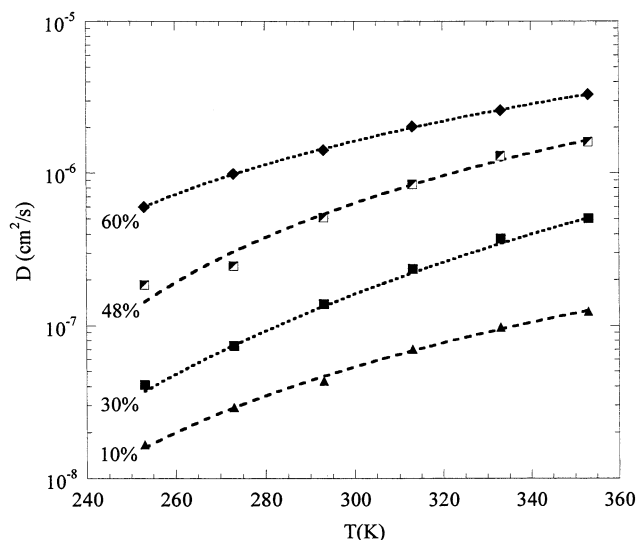


Figure 7. Representative WLF plots of the temperature dependence of the self-diffusion constants of DMMP as a function of temperature at a given concentration.

Table 3. WLF Parameters for DMMP

wt %	ϕ	$f(\phi_s)/B_d$	$\alpha(\phi_s)/B_d \times 10^4$
10	0.46	0.14	3.7
20	0.53	0.14	5.5
30	0.62	0.13	5.2
48	0.74	0.18	9.5
60	0.82	0.34	21

$\alpha(\phi_s)$ is the fractional free volume expansion factor, B_d is the minimum hole size needed to allow the molecule in question to undergo displacement, and T_0 is the reference temperature. Some representative diffusion constants plotted as a function of temperature at a given concentration and the corresponding fits according to eq 5 are shown in Figure 7. The parameters of the fit are given in Table 3.

Although free volume theory is not applicable given the nature of the concentration dependence, the WLF parameters are interesting. Below 30 wt % DMMP ($\phi_s = 0.62$ and less in Table 3), $f(\phi_s)/B_d$ and $\alpha(\phi_s)/B_d$ have values typical for a low molecular weight solvent in a polymer and comparable to those determined for water in Nafion. Above 30 wt %, there is an increase in both parameters to values that are rather too large for the typical solvent–polymer system. Again, the jump in the parameters is at the point where the second larger domain is becoming a significant part of the morphology. The larger WLF parameters were similar to those of ethanol in Nafion where there was also evidence for structural rearrangement and larger domains.

Discussion

DMMP is very soluble in Nafion, but fluorine-19 NMR shows only the pendant group domain is plasticized. Thus, DMMP is primarily considered to sorb into this domain. Since the solubility is so high, this domain becomes larger in volume fraction than the backbone domain as concentration is increased. Fluorine-19 spin diffusion experiments show the presence of a second, larger pendant group domain developing as concentration is raised as well as the persistence of the smaller domain similar in size to that present in dry Nafion. Interestingly, the smaller domain associated with the original Nafion morphology is never completely elimi-

nated. In the scattering data of Gebel,⁶ there was a crystalline component of the poly(fluoroethylene) backbone domain which remained even in solutions of Nafion in water produced at high temperatures. In the DMMP case where only low temperatures are used, perhaps some of the original morphology is locked into place by crystalline or rigid backbone components while more mobile or amorphous components undergo morphological change to produce the larger domain structure.

Nafion is a random copolymer of perfluoroethylene units and ionomeric units. The crystalline part of the backbone domains are likely to contain few of the large ionomeric units. The more amorphous components of the backbone domain are likely to have more associated ionomeric units. The pendant groups form domains, but the adjacent backbone domains are likely to be amorphous following this line of argument. As DMMP concentration is raised, it is this part of the system which may be more able to undergo the morphological change which is observed. The more rigid or crystalline backbone regions may act as the constraint on the nearby pendant group domains that are limited in size and only swell to a level of about 10 wt % DMMP. Thus, the surroundings of the smaller pendant group domain place limits on the level of swelling while other regions with less rigid surroundings can continue to swell.

The larger domain structure must have a larger interface given the shape of the spin diffusion curves. This is also reasonable given the nature of the random copolymer nature of Nafion. As a larger domain is developed with increasing DMMP content, it will be more difficult to have good segregation between backbone and pendant groups. The best compromise would be a thickening interface which is supported by the spin diffusion data. In dry Nafion there is a sharper interface, and the smaller pendant group domain largely retains this sharper interface.

The diffusion data also undergo a transition with a rapid increase in translational mobility as the pendant group plus DMMP phase becomes the majority of the system. The larger phase structure presents less obstruction associated with the more impenetrable fluorocarbon backbone domain so an increase in such mobility seems reasonable. Another way to state this is that the space accessible to DMMP is better interconnected in the larger domain morphology.

Free volume theory could not be applied to characterize the concentration dependence of the diffusion. It is actually surprising that such an approach worked for water in Nafion given the morphological complexity of the system. However, swelling with water at room temperature does not lead to the development of a new morphology as does DMMP where the change in morphology led to an unusual concentration dependence. On the other hand, a traditional WLF approach could summarize the temperature dependence even if it was some average over the two morphologies present at high concentration. The WLF parameters also change at the point where the new morphology begins to become important.

Conclusions

The combined study of translational diffusion and structure for DMMP in Nafion provides a number of mutually supportive insights into a rather complicated situation. Nafion without DMMP has a complex morphology involving ionic clusters, crystalline and amorphous backbone domains, and a pendant group domain. At the outset of this investigation it is hard to guess where the DMMP would be located as it is sorbed into Nafion. The results of the NMR measurements are clear. The backbone domain remains unplasticized by DMMP while the pendant group domain is given reorientational mobility and develops a new morphology. The new morphology is larger in size and leads to a sharp rise in translational mobility with increasing DMMP concentration. The changes of the self-diffusion constant of DMMP with concentration are only comprehensible when meshed with the structural changes which are observed in the same concentration range. The change in morphological structure at high levels of DMMP is likely enabled by the high degree of mobility imparted to the pendant group domain. Spatial reorganization of the highly swollen, mobile pendant groups is only restrained by the backbone units which are still located in rather rigid domains unaffected by the presence of DMMP.

Acknowledgment. This work was supported by the Army Research Office, Grant DAAD19-00-1-0430.

References and Notes

- (1) *Ionomers*; Tant, M. R., Mauritz, K. A., Wilkes, G. L., Eds.; Blackie Academic & Professional: London, 1997.
- (2) *Perfluorinated Ionomer Membranes*; Eisenberg, A., Yeager, H., Eds.; ACS Symposium Series 180; American Chemical Society: Washington, DC, 1982.
- (3) Gierke, T. D.; Hsu, W. Y. In *Perfluorinated Ionomer Membranes*; Eisenberg, A., Yeager, H., Eds.; ACS Symposium Series 180; American Chemical Society: Washington, DC, 1982.
- (4) Meresi, G.; Wang, Y.; Bandis, A.; Inglefield, P. T.; Jones, A. A.; Wen, W.-Y. *Polymer* **2001**, *42*, 6153.
- (5) Eisenberg, A.; Hird, B.; Moore, R. B. *Macromolecules* **1990**, *23*, 4098.
- (6) Gebel, G. *Polymer* **2000**, *41*, 5829.
- (7) Rubatat, L.; Rollet, A. L.; Gebel, G.; Diat, O. *Macromolecules* **2002**, *35*, 4050.
- (8) Chomakova-Haefke, M.; Nyffenegger, R.; Schmidt, E. *Appl. Phys. A: Mater. Sci. Process.* **1994**, *59*, 151.
- (9) Gong, X.; Bandis, A.; Tao, A.; Meresi, G.; Wang, Y.; Inglefield, P. T.; Jones, A. A.; Wen, W.-Y. *Polymer* **2001**, *42*, 6485.
- (10) Mitra, P. P.; Sen, P. N.; Schwartz, L. M.; LeDoussal, P. *Phys. Rev. Lett.* **1992**, *68*, 3555.
- (11) Callaghan, P. T. *Principles of Nuclear Magnetic Resonance Microscopy*; Oxford University Press: New York, 1991.
- (12) VanderHart, D. L.; McFadden, G. B. *Solid State NMR* **1996**, *7*, 45.
- (13) Weigand, F.; Demco, D. E.; Blemich, B.; Spiess, H. W. *J. Magn. Reson. A* **1996**, *120*, 190.
- (14) Demco, D. E.; Johansson, A.; Tegenfeldt, J. *Solid State NMR* **1995**, *4*, 13.

MA021777A